Supplementary material

Supplementary movies

Movie 1. MZ*nanog* mutant show proper cleavages during first 3 hours of development and abnormal epiboly. The movie starts when wild-type (right) and MZ*nanog* (left) embryos are at 4-cell stage. For visualization, the embryos were injected with SYTOX Green at 1-cell stage. Following the cleavages from 4-cell to 1k-cell stage, there is no recognizable difference between wild-type and mutant embryos. Nanog mutants undergo the cleavages with the same timing and with the same number of cycles, which we confirmed by counting cell cycles (data not shown). The movie stops after 21 hours when the mutant embryo died through yolk lysis. The movie was recorded at room temperature.

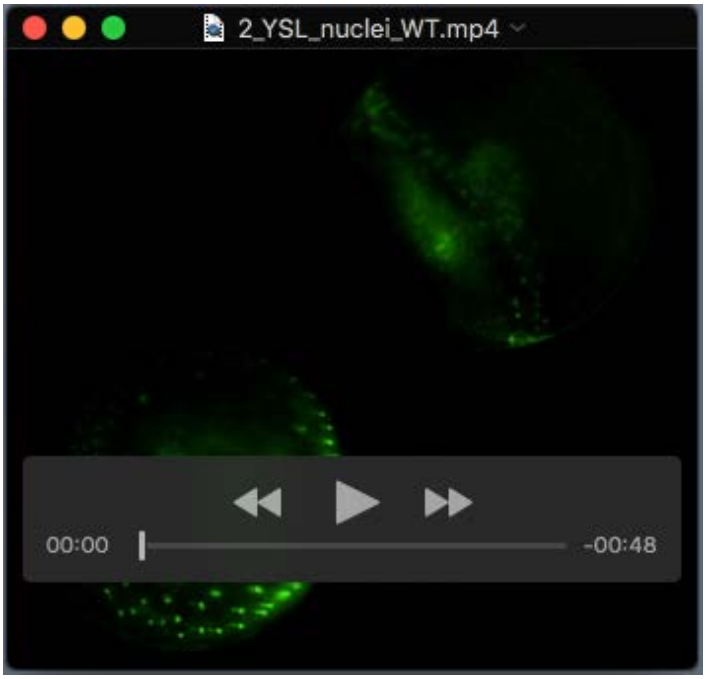

Movie 2. YSL nuclei movements in wild type embryos. Embryos were injected with SYTOX Green at 1-cell stage to visualize the YSL. The injected embryos were embedded in low melting agarose to show the animal (below) and lateral (above) view and the movie was started when they, reached oblong stage. Frames were taken every 3 min. Note the changing distribution of the YSL nuclei: YSL nuclei first stay as 3 rows in the periphery of the yolk, then the nuclei aligned at one row and as doming starts some YSL nuclei migrate to the middle.

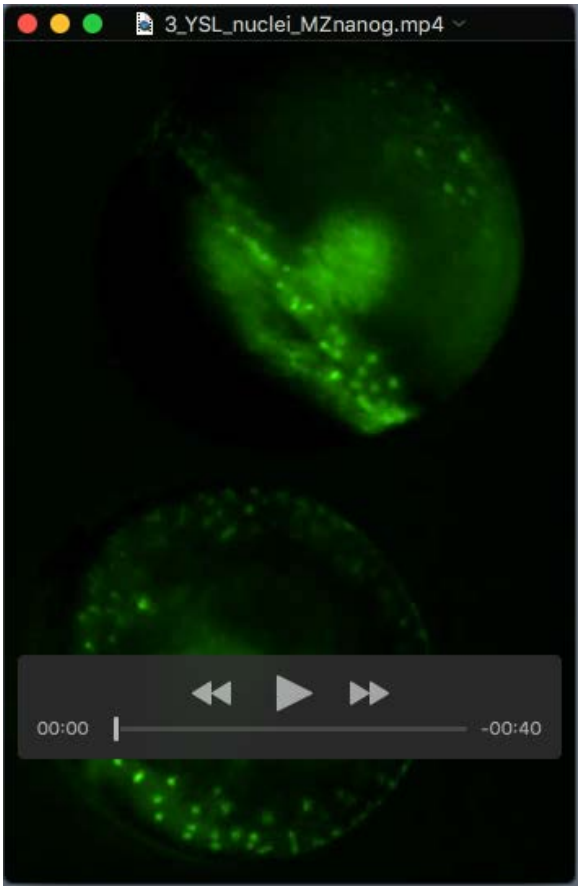

Movie 3. YSL nuclei movement in MZ*nanog* embryos is impaired. Embryos were injected with SYTOX Green at 1-cell stage to visualize YSL. The movie was started when the control wild type embryos reached oblong stage, frames were taken every 3 min. Embryo below is in animal view, embryo above is in lateral view. Note that no nuclei movement or doming is visible until the yolk lysis.

Supplementary figures

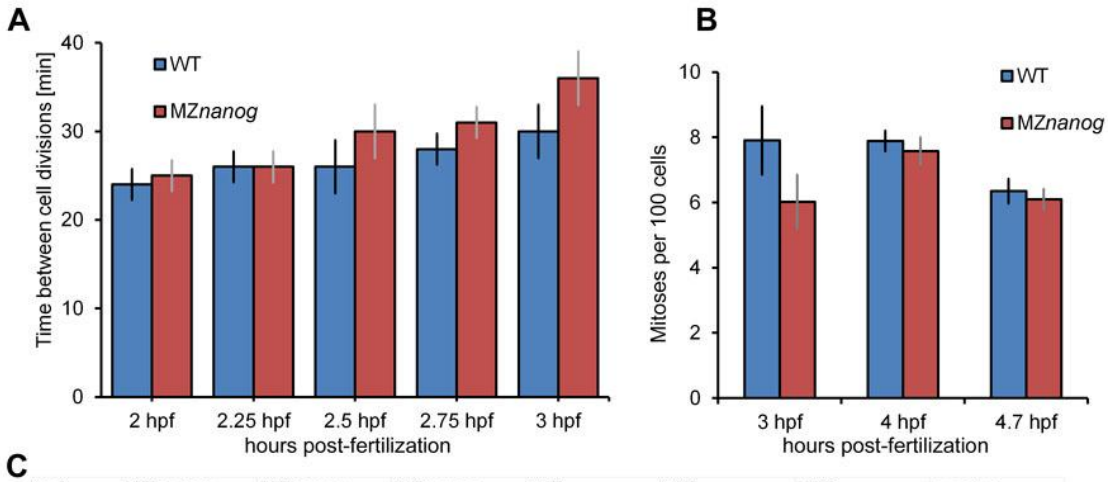

C

hpf	MZ*nanog* n embryos	MZ*nanog* n mitotic	MZ*nanog* n total cells	WT n embryos	WT n mitotic	WT n total cells	p-value MZ*nanog*-WT
3	32	163	2563	30	218	2838	0.167
4	37	694	9563	34	717	9130	0.519
4.7	19	345	5707	25	483	7675	0.682

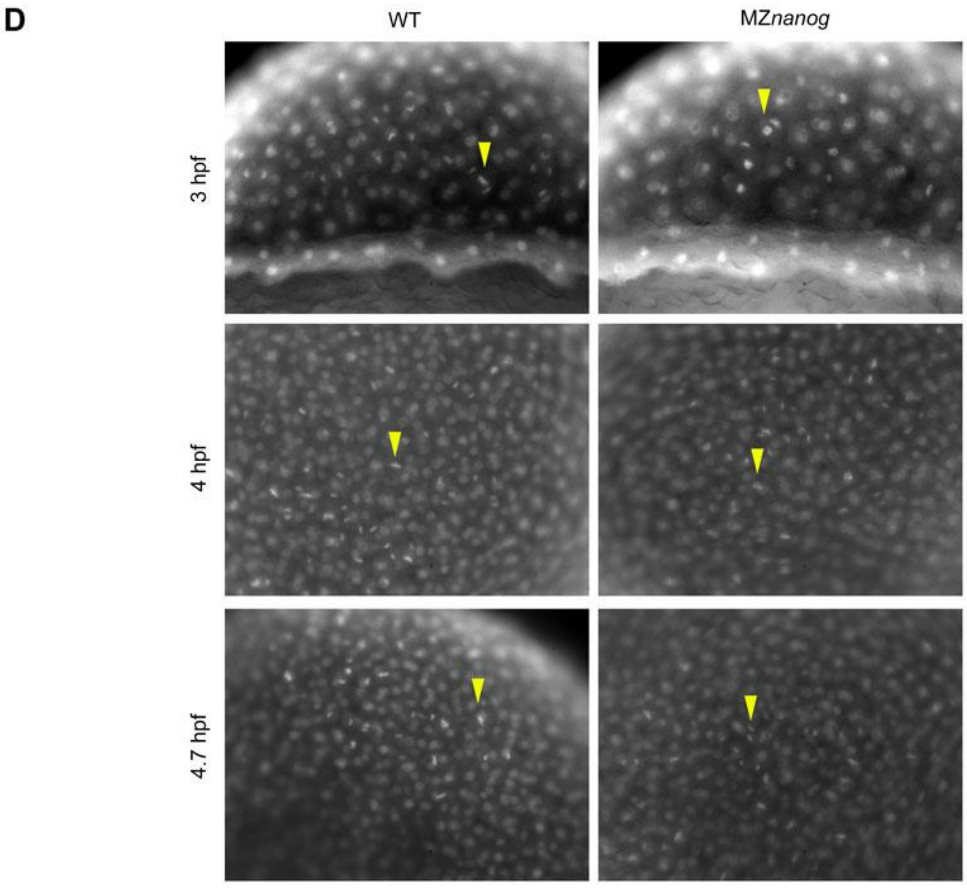

Fig. S1. Pre-ZGA and post-ZGA cell division rates in WT and MZ*nanog* are not significantly different. (A) Timing of pre-MBT cleavages in wild-type and MZ*nanog* embryos.

Y-axis: Time between cell divisions (from 2 – 3 hpf) was estimated from 3 time-lapse records, including Supplementary Movie 1. Error bars: standard deviation, n=3. (B-D) Mitotic rates of WT and MZ*nanog* at 3 hpf, 4 hpf and 4.7 hpf (see Materials and Methods). (D) Y axis: number of mitoses per 100 cells, Error bars: SEM. (C) Summary table for mitotic cell and total cell counts (see Table S1 for all counts per embryo). (D) Example images of each stage and genotype, yellow arrowheads show mitotic cells. Scale bar corresponds to 125 µm.

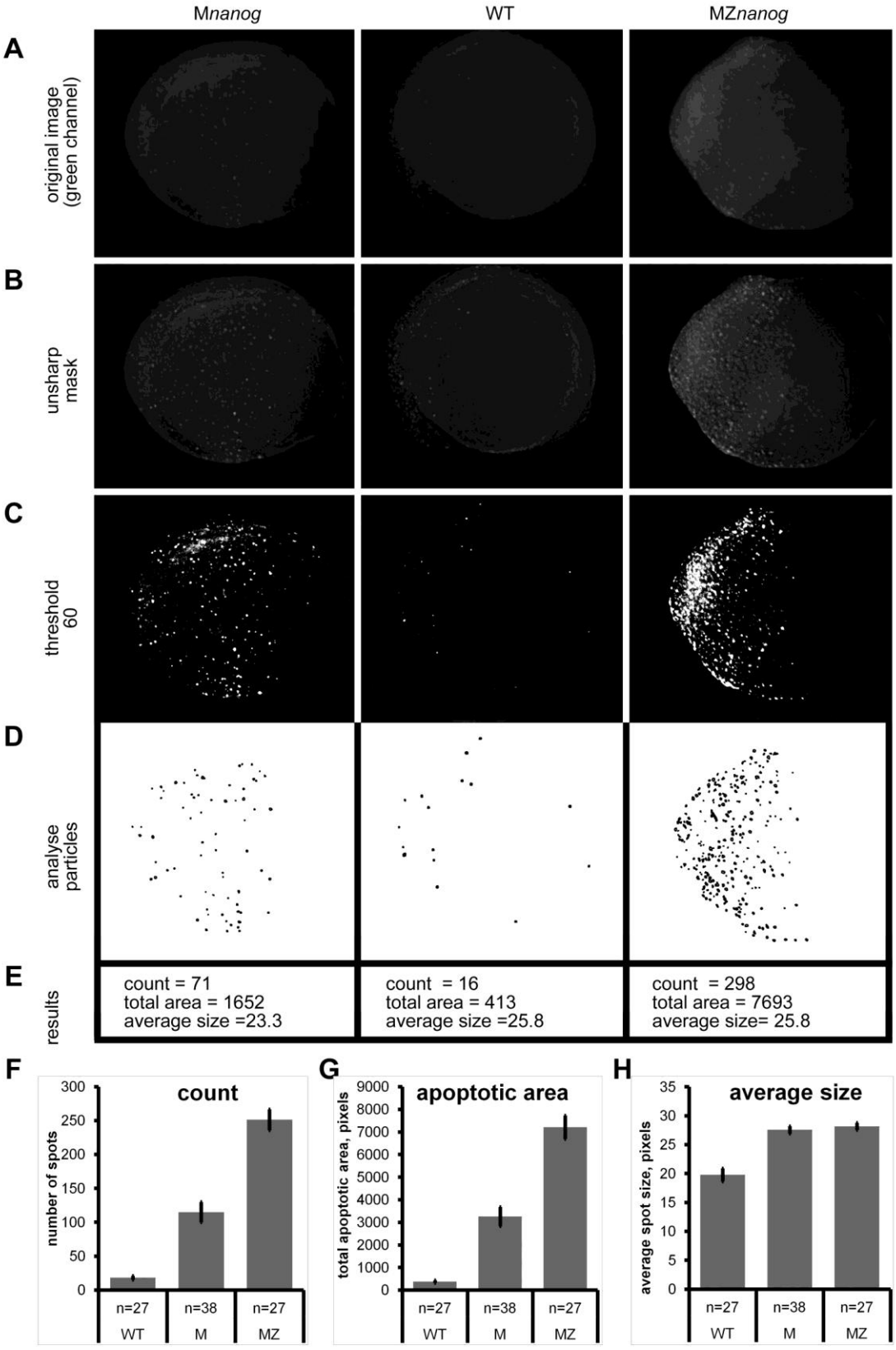

Fig. S2. Image processing pipeline for comparing relative cell death rates within the experiment. (A-E) Processing of 3 images (M*nanog*, WT, MZ*nanog*) shown at Fig. 2 of the

main text is taken as example. Embryos were stained and images taken as described in “Materials and Methods”. Then images in TIFF format (A) were sharpened in Adobe Photoshop with “Unsharp Mask” Filter (B), and thresholded in ImageJ (C). The spots of 4-100 pixels size visualized in (D) representing clusters of dead cells or single cells were taken as a measure of dead cells per embryo. Count, total area and average size of the spots per image (E) was recorded for 20-40 images per condition. (F-H) statistics of count (F), total area (G) and average size (H) for WT, M*nanog* and MZ*nanog* using threshold 60, which gave in the closest values for average spot size in different experimental groups (H). Total area was normalized to the average MZ*nanog* value and used as a relative measure for the amount of cell death between experimental conditions (genotypes or treatments). Scale bar in A-D indicates 100 µm.

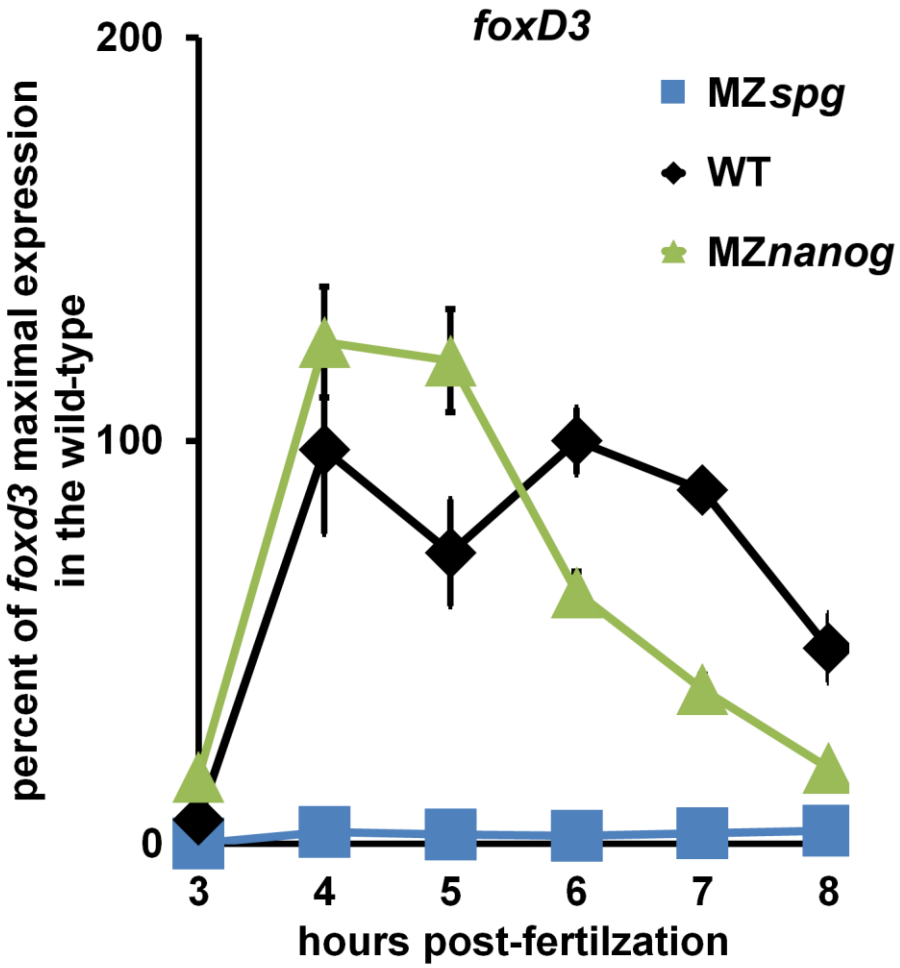

Fig. S3. Expression of *foxD3* in the wild-type, MZ*nanog* and MZ*spg* embryos. Graph shows *foxD3* expression time-curve generated by quantitative real time PCR in the wild-type, MZ*nanog*, and MZ*spg*. Embryos were collected in 1 hour intervals from 3 hpf till 8 hpf. All expression values were normalized to maximal expression in the wild-type. Note that *foxD3* expression starts at the same time in the MZ*nanog* and in the wild-type, while in MZ*spg* *foxD3* expression is missing as reported before (Onichtchouk et al., 2010).

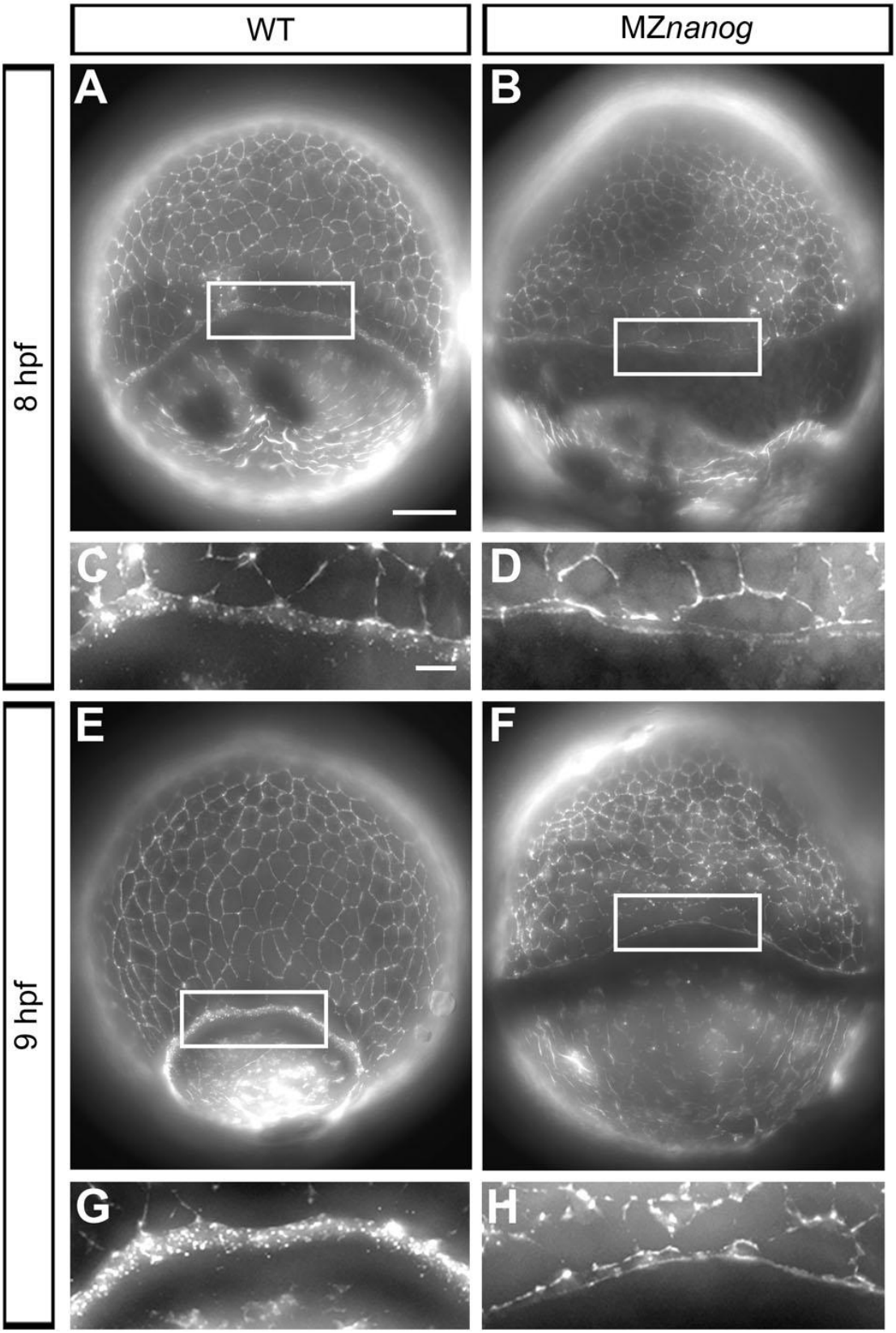

Fig. S4. F-actin ring does not form and EVL-YSL border does not constrict in MZ*nanog*.
(A-H) F-actin ring visualization by rhodamin-phalloidin staining of wild-type and MZ*nanog*

embryos at 8 hpf and 9 hpf (75% epiboly of wild-type control and 90% epiboly of wild-type control), as indicated. The higher magnification views of boxed areas show the endocytic vesicles in the wild-type (C,G) which are missing in MZ*nanog* (D,H). Note that at the 8 hpf higher magnification view two faint actin bands are visible in MZ*nanog* - one in the EVL cells and one in the YSL (D). This may indicate detachment of the marginal EVL cells from the YSL. Scale bars correspond to 100 µm in A,B,E,F and 20 µm in C,D,G,H.

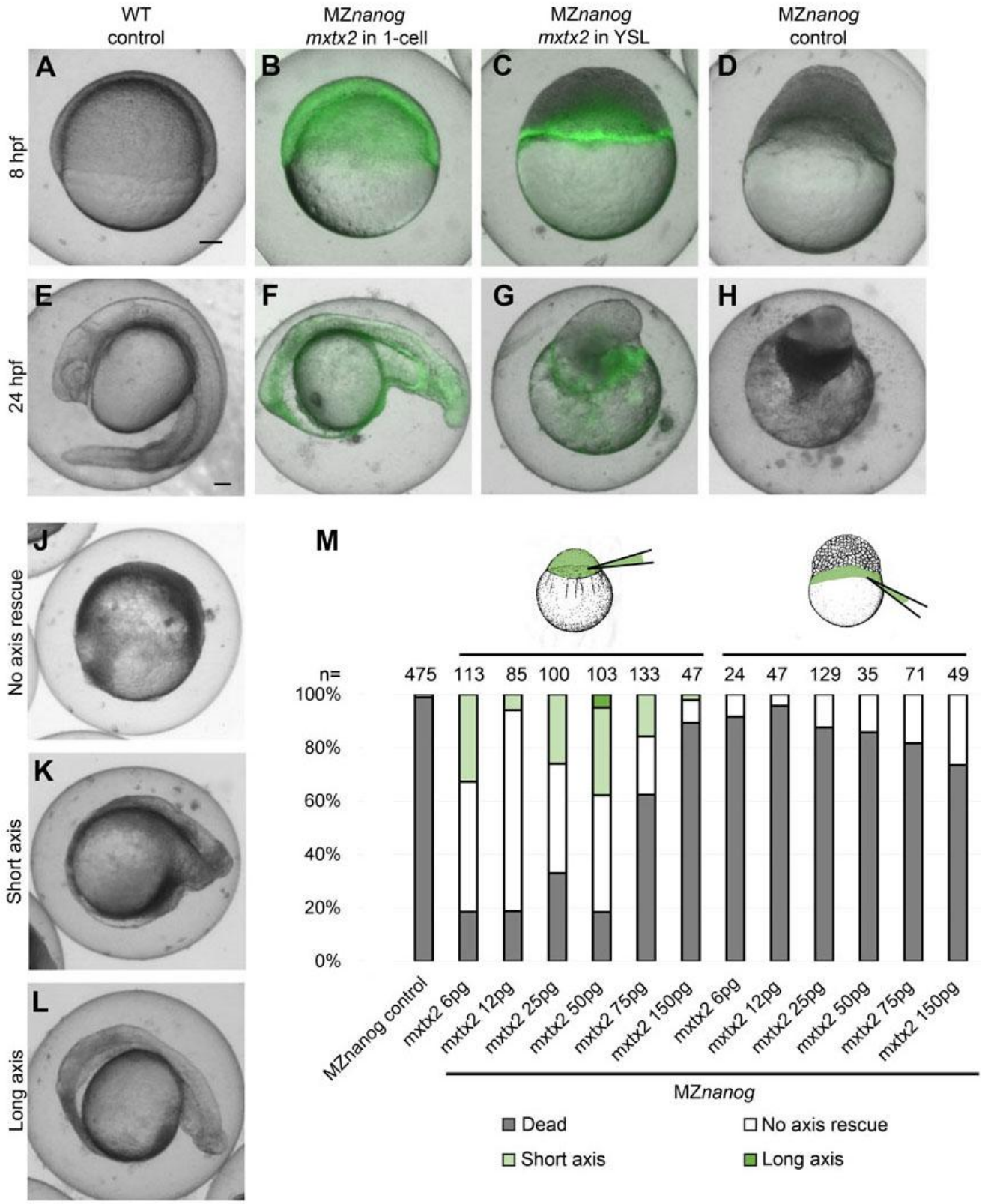

Fig. S5. *mxtx2* mRNA injection at 1 cell stage but not to the YSL rescues epiboly in MZ*nanog* embryos. (A-H) Representative embryo phenotypes from single rescue experiment: *mxtx2* mRNA was co-injected with Alexa488 dextran (green) in the YSL (C, G) or

in 1-cell stage (B,F) of MZ*nanog* embryos. Live images in DIC and green fluorescence were taken from injected and non-injected wild-type and MZ*nanog* at 75% epiboly of the wild-type control (8 hpf) and 24 hpf, as indicated. Note that MZ*nanog* embryos injected into 1-cell stage restored epiboly (B) and some of them formed the partial body axis with tail (F). The phenotypes of YSL-injected MZ*nanog* embryos were not distinguishable from non-injected MZ*nanog* at 8 hpf (compare C and D) and 24 hpf (G and H). Scale bars in A-H indicate 100 µm. (J-L) Phenotypic classes used for scoring the rescued phenotypes in *mxtx2* experiment at 24 hpf: no axis rescue (J), short axis rescue (K) or long rescue (L). (M) Rescue statistics after 24 hpf, six concentrations of *mxtx2* mRNA (indicated below the graph in pg per embryo) were used for injections of MZ*nanog* embryos at the 1-cell stage and to the YSL at the 512-cell stage, as indicated above the graph. Phenotypic classes used for scoring are shown in J-L. Numbers of injected or non-injected embryos are indicated above the bars.

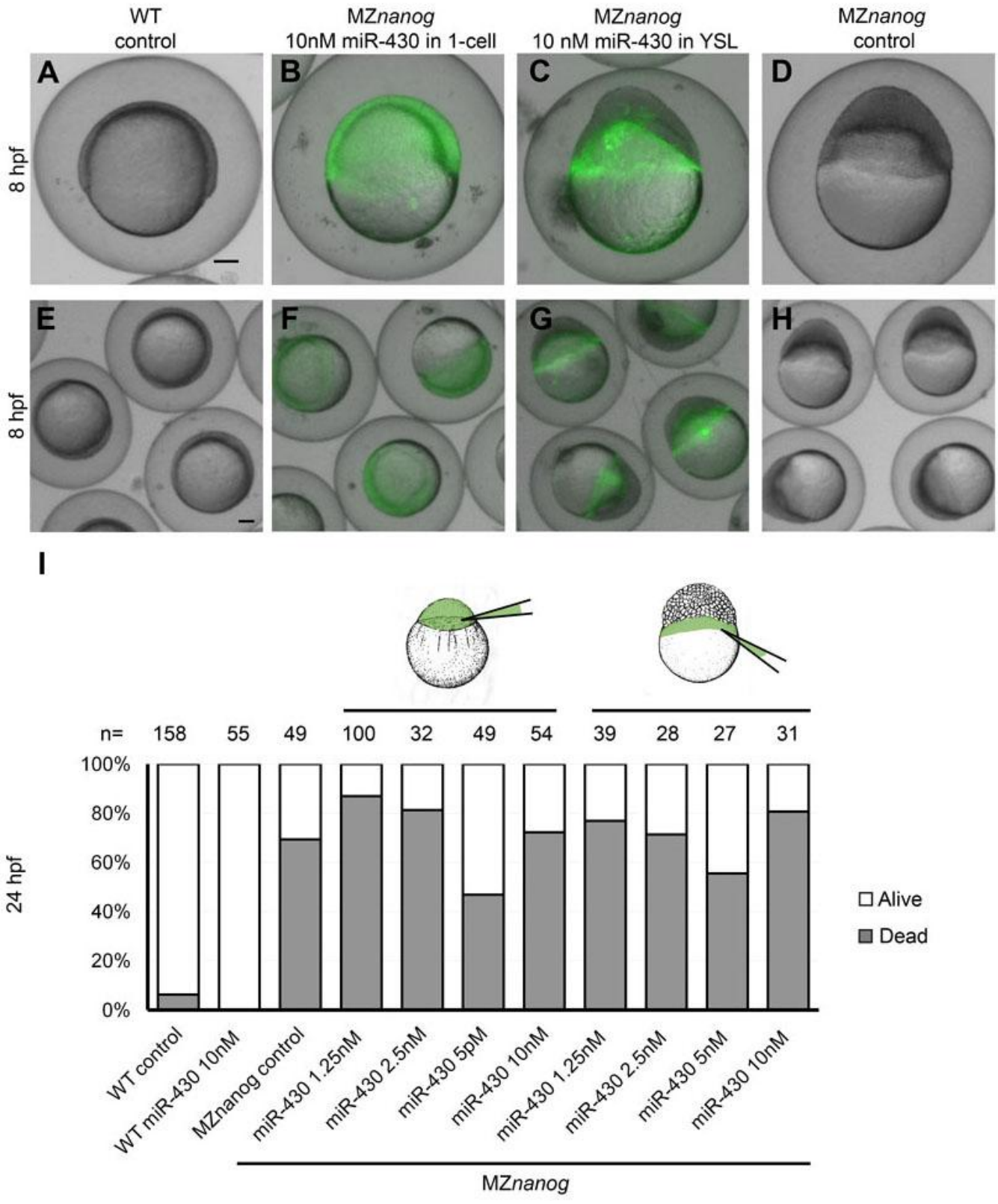

Fig. S6. miR-430 injection at 1-cell stage but not into the YSL rescues epiboly in MZ*nanog* embryos. (A-D) Representative embryo phenotypes and (E-H) groups of embryos from single rescue experiment: miR-430 was co-injected with Alexa488 dextran (green) in the

YSL (C, G) or in 1-cell stage (B,F) of MZ*nanog* embryos. Live images in DIC and green fluorescence were taken from injected and non-injected WT and MZ*nanog* at 75% epiboly of wild-type control (8 hpf). Note that MZ*nanog* embryos injected into 1-cell stage restored epiboly (compare B,F with D,H) while the phenotype of YSL-injected MZ*nanog* embryos were not distinguishable from non-injected MZ*nanog* at 8 hpf (compare C,G with D,H). (I) miR-430 injected MZ*nanog* embryos did not form embryonic axes and death rates at 24 hpf were not significantly improved. (I) Rescue statistics after 24 hpf, four concentrations of miR-430 (indicated below the graph) were used for injections of MZ*nanog* embryos at the 1-cell stage and to the YSL at the 512-cell stage, as indicated above the graph.

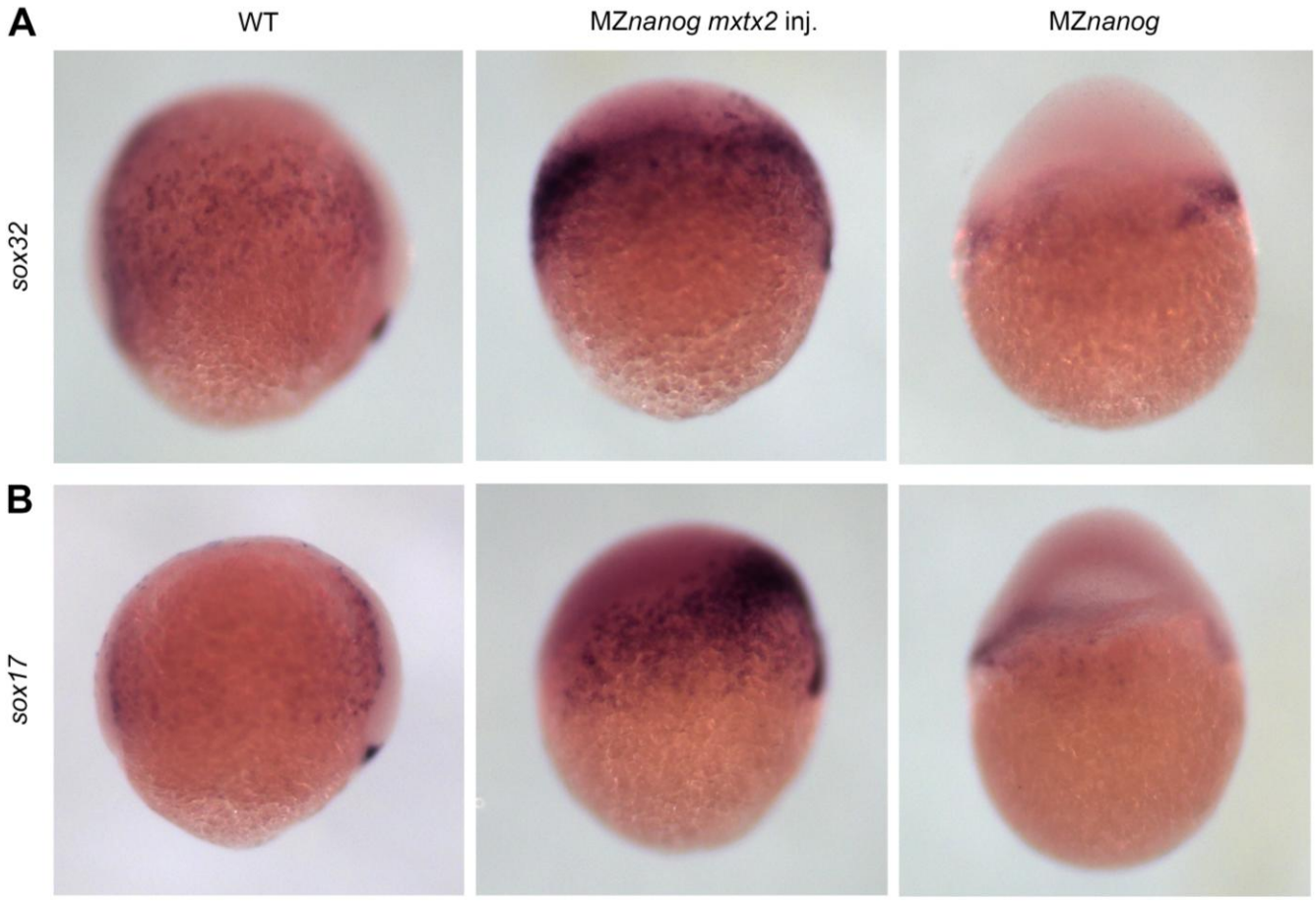

Fig. S7. Excessive endoderm formation in *mxtx2*-injected MZ*nanog* embryos. *In-situ* hybridization of 8 hpf embryos with *sox32* (A) or *sox17* (B) probe, lateral views. MZ*nanog* embryos were injected with 12 pg/embryo of *mxtx2* mRNA at 1-cell stage, or left non-injected as indicated above. Non-injected wild-type embryos were used as staining controls. Note that the amount of *sox32*- and *sox17*-positive cells in *mxtx2*-injected MZ*nanog* visibly exceeds that number in MZ*nanog* control and even in the wild-type stage-matched embryo.

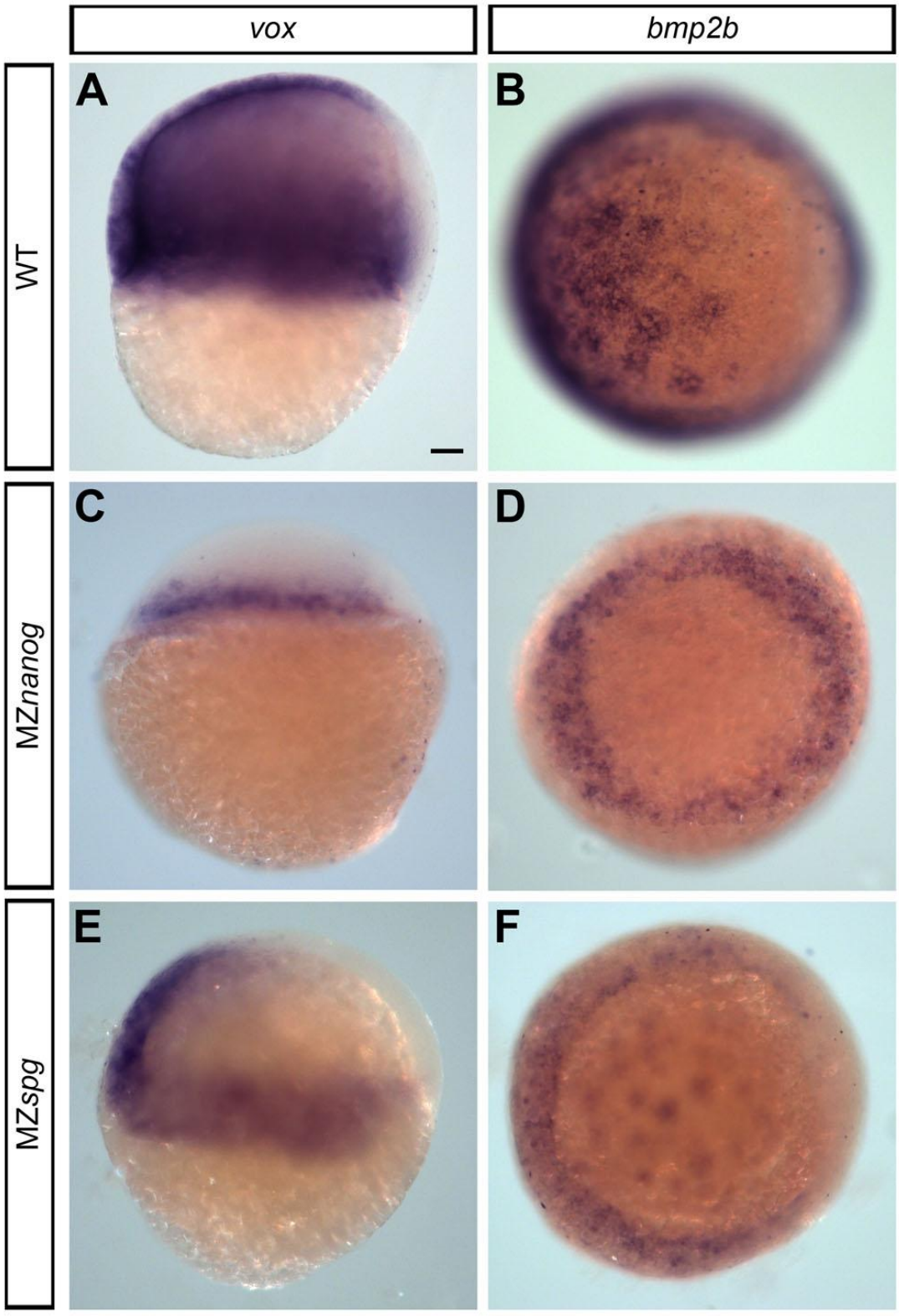

Fig. S8. Nanog is required for expression of ventral genes *bmp2b* and *vox.* *In situ* hybridization for *vox* (A,C,E) and *bmp2b* (B,D,F) at a closer look. Expression of both genes is

reduced in the mesoderm and missing from the ectoderm of MZ*nanog*, while in MZ*spg* expression in both tissues is reduced, but detectable. Scale bar corresponds to 100 µm.

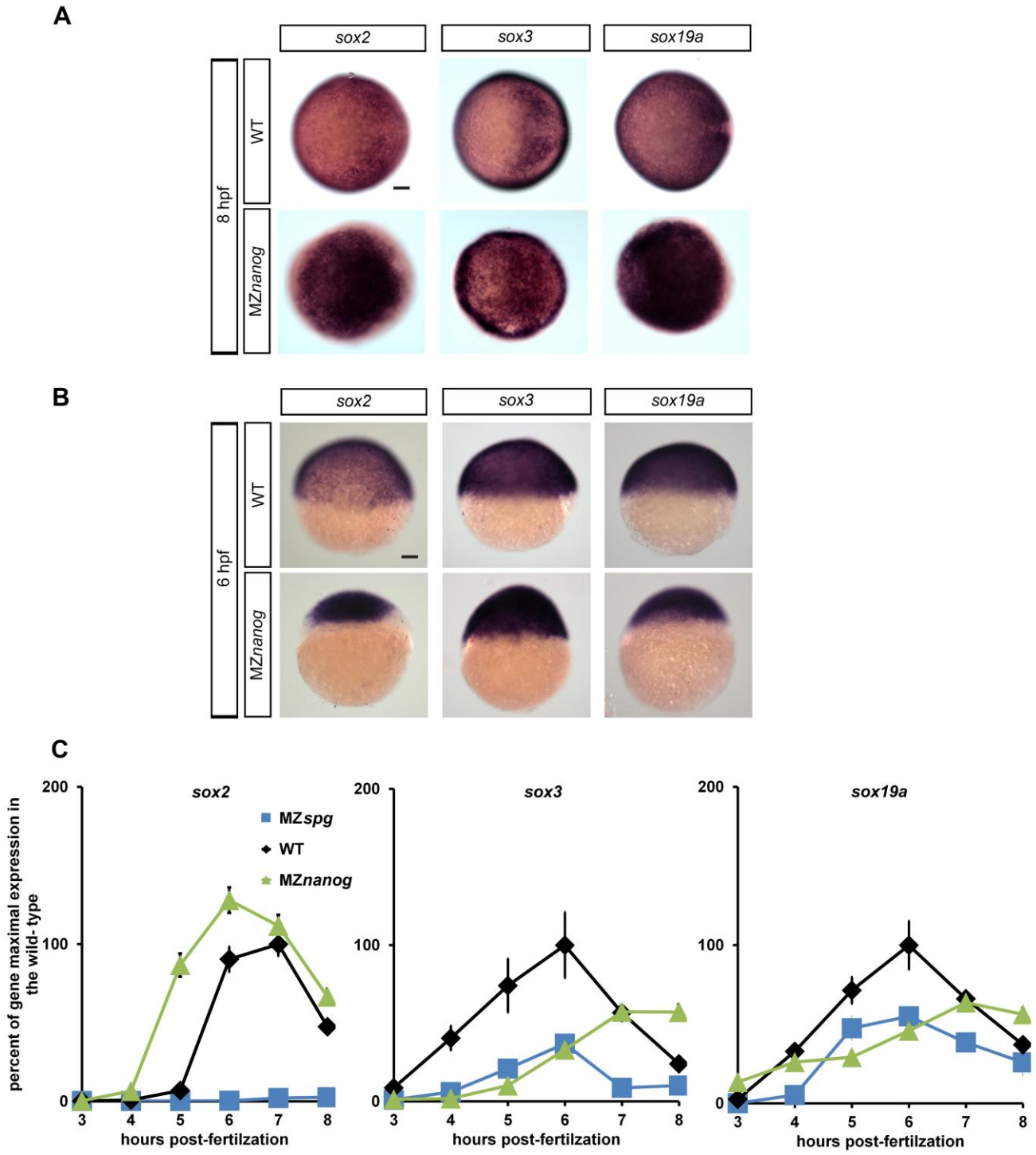

Fig. S9. Expression of *sox2*, *sox3* and *sox19a* in the wild-type and MZ*nanog* embryos. (A) *In situ* hybridization at 8 hpf, animal view, dorsal to the right. Note that neural restriction of *soxb1* genes occurs in the wild-type but not in MZ*nanog*. (B) *In situ* hybridization at 6 hpf, lateral view. (C) Graph shows time-curve generated by quantitative real time PCR on wild-

type, MZ*nanog*, and MZ*spg*. Embryos were collected in 1 hour intervals from 3 hpf till 8 hpf. All expression values were normalized to maximal expression in the wild-type. Note that *soxb1* genes change differently compared to the wild-type: *sox2* is moderately increased and expression starts 1 hour earlier, *sox3* expression starts later and is initially reduced, *sox19a* expression starts at the same time but is reduced at 5 and 6 hpf. At 8 hpf the levels of *sox3* and *sox19a* in MZ*nanog* exceed the levels in the wild-type, which is probably due to the absence of neural restriction in MZ*nanog* (see A).

Supplementary tables

Table S1. Numbers of counted mitotic and total cells at MZ*nanog* and WT embryos. Related to Fig. S1 and Materials and Methods.

genotype	stage	embryo nr	mitotic cells	all nuclei	ratio mitotic/all
MZnanog	3 hpf	1	10	91	0.10989
MZnanog	3 hpf	2	7	57	0.12281
MZnanog	3 hpf	3	4	79	0.05063
MZnanog	3 hpf	4	10	89	0.11236
MZnanog	3 hpf	5	12	113	0.10619
MZnanog	3 hpf	6	0	58	0
MZnanog	3 hpf	7	0	90	0
MZnanog	3 hpf	8	1	51	0.01961
MZnanog	3 hpf	9	3	61	0.04918
MZnanog	3 hpf	10	5	84	0.05952
MZnanog	3 hpf	11	6	97	0.06186
MZnanog	3 hpf	12	4	47	0.08511
MZnanog	3 hpf	13	12	98	0.12245
MZnanog	3 hpf	14	0	51	0
MZnanog	3 hpf	15	0	85	0
MZnanog	3 hpf	16	0	80	0
MZnanog	3 hpf	17	0	63	0
MZnanog	3 hpf	18	5	57	0.08772
MZnanog	3 hpf	19	8	65	0.12308
MZnanog	3 hpf	20	5	67	0.07463
MZnanog	3 hpf	21	9	86	0.10465
MZnanog	3 hpf	22	16	108	0.14815
MZnanog	3 hpf	23	5	110	0.04545
MZnanog	3 hpf	24	0	75	0
MZnanog	3 hpf	25	6	69	0.08696
MZnanog	3 hpf	26	9	94	0.09574

MZnanog	3 hpf	27	10	131	0.07634
MZnanog	3 hpf	28	0	72	0
MZnanog	3 hpf	29	7	86	0.0814
MZnanog	3 hpf	30	1	64	0.01563
MZnanog	3 hpf	31	3	96	0.03125
MZnanog	3 hpf	32	5	89	0.05618
WT	3 hpf	1	12	65	0.18462
WT	3 hpf	2	11	97	0.1134
WT	3 hpf	3	2	100	0.02
WT	3 hpf	4	3	77	0.03896
WT	3 hpf	5	5	97	0.05155
WT	3 hpf	6	14	105	0.13333
WT	3 hpf	7	5	113	0.04425
WT	3 hpf	8	1	86	0.01163
WT	3 hpf	9	4	99	0.0404
WT	3 hpf	10	3	80	0.0375
WT	3 hpf	11	2	102	0.01961
WT	3 hpf	12	6	85	0.07059
WT	3 hpf	13	7	100	0.07
WT	3 hpf	14	8	101	0.07921
WT	3 hpf	15	4	78	0.05128
WT	3 hpf	16	3	105	0.02857
WT	3 hpf	17	1	93	0.01075
WT	3 hpf	18	8	107	0.07477
WT	3 hpf	19	3	96	0.03125
WT	3 hpf	20	11	54	0.2037
WT	3 hpf	21	11	91	0.12088
WT	3 hpf	22	19	110	0.17273
WT	3 hpf	23	7	111	0.06306
WT	3 hpf	24	2	87	0.02299
WT	3 hpf	25	3	88	0.03409
WT	3 hpf	26	13	122	0.10656
WT	3 hpf	27	14	81	0.17284
WT	3 hpf	28	15	88	0.17045

WT	3 hpf	29	17	109	0.15596
WT	3 hpf	30	4	111	0.03604
MZnanog	4 hpf	1	21	290	0.07241
MZnanog	4 hpf	2	18	296	0.06081
MZnanog	4 hpf	3	21	246	0.08537
MZnanog	4 hpf	4	17	303	0.05611
MZnanog	4 hpf	5	13	227	0.05727
MZnanog	4 hpf	6	17	222	0.07658
MZnanog	4 hpf	7	18	213	0.08451
MZnanog	4 hpf	8	17	356	0.04775
MZnanog	4 hpf	9	9	227	0.03965
MZnanog	4 hpf	10	12	309	0.03883
MZnanog	4 hpf	11	27	244	0.11066
MZnanog	4 hpf	12	21	212	0.09906
MZnanog	4 hpf	13	11	200	0.055
MZnanog	4 hpf	14	23	258	0.08915
MZnanog	4 hpf	15	22	291	0.0756
MZnanog	4 hpf	16	13	214	0.06075
MZnanog	4 hpf	17	22	283	0.07774
MZnanog	4 hpf	18	14	240	0.05833
MZnanog	4 hpf	19	28	274	0.10219
MZnanog	4 hpf	20	16	285	0.05614
MZnanog	4 hpf	21	28	339	0.0826
MZnanog	4 hpf	22	15	277	0.05415
MZnanog	4 hpf	23	16	192	0.08333
MZnanog	4 hpf	24	22	165	0.13333
MZnanog	4 hpf	25	25	238	0.10504
MZnanog	4 hpf	26	16	255	0.06275
MZnanog	4 hpf	27	30	242	0.12397
MZnanog	4 hpf	28	19	342	0.05556
MZnanog	4 hpf	29	15	183	0.08197
MZnanog	4 hpf	30	20	255	0.07843
MZnanog	4 hpf	31	14	217	0.06452
MZnanog	4 hpf	32	26	271	0.09594

MZnanog	4 hpf	33	14	272	0.05147
MZnanog	4 hpf	34	15	366	0.04098
MZnanog	4 hpf	35	19	240	0.07917
MZnanog	4 hpf	36	19	234	0.0812
MZnanog	4 hpf	37	21	285	0.07368
WT	4 hpf	1	14	175	0.08
WT	4 hpf	2	33	368	0.08967
WT	4 hpf	3	12	151	0.07947
WT	4 hpf	4	7	97	0.07216
WT	4 hpf	5	29	280	0.10357
WT	4 hpf	6	28	299	0.09365
WT	4 hpf	7	24	226	0.10619
WT	4 hpf	8	13	245	0.05306
WT	4 hpf	9	12	273	0.04396
WT	4 hpf	10	21	228	0.09211
WT	4 hpf	11	26	285	0.09123
WT	4 hpf	12	15	210	0.07143
WT	4 hpf	13	33	280	0.11786
WT	4 hpf	14	19	212	0.08962
WT	4 hpf	15	22	300	0.07333
WT	4 hpf	16	25	312	0.08013
WT	4 hpf	17	13	293	0.04437
WT	4 hpf	18	24	312	0.07692
WT	4 hpf	19	25	273	0.09158
WT	4 hpf	20	16	350	0.04571
WT	4 hpf	21	17	223	0.07623
WT	4 hpf	22	14	227	0.06167
WT	4 hpf	23	14	203	0.06897
WT	4 hpf	24	23	311	0.07395
WT	4 hpf	25	18	275	0.06545
WT	4 hpf	26	22	213	0.10329
WT	4 hpf	27	19	211	0.09005
WT	4 hpf	28	25	294	0.08503
WT	4 hpf	29	23	297	0.07744

WT	4 hpf	30	32	403	0.0794
WT	4 hpf	31	21	288	0.07292
WT	4 hpf	32	30	409	0.07335
WT	4 hpf	33	31	351	0.08832
WT	4 hpf	34	17	256	0.06641
MZnanog	4.7 hpf	1	26	358	0.07263
MZnanog	4.7 hpf	2	13	299	0.04348
MZnanog	4.7 hpf	3	16	219	0.07306
MZnanog	4.7 hpf	4	14	203	0.06897
MZnanog	4.7 hpf	5	1	280	0.00357
MZnanog	4.7 hpf	6	15	214	0.07009
MZnanog	4.7 hpf	7	25	411	0.06083
MZnanog	4.7 hpf	8	23	318	0.07233
MZnanog	4.7 hpf	9	18	290	0.06207
MZnanog	4.7 hpf	10	14	313	0.04473
MZnanog	4.7 hpf	11	15	261	0.05747
MZnanog	4.7 hpf	12	16	270	0.05926
MZnanog	4.7 hpf	13	16	212	0.07547
MZnanog	4.7 hpf	14	20	317	0.06309
MZnanog	4.7 hpf	15	29	419	0.06921
MZnanog	4.7 hpf	16	29	404	0.07178
MZnanog	4.7 hpf	17	15	188	0.07979
MZnanog	4.7 hpf	18	16	384	0.04167
MZnanog	4.7 hpf	19	24	347	0.06916
WT	4.7 hpf	1	12	323	0.03715
WT	4.7 hpf	2	14	319	0.04389
WT	4.7 hpf	3	28	260	0.10769
WT	4.7 hpf	4	13	259	0.05019
WT	4.7 hpf	5	25	349	0.07163
WT	4.7 hpf	6	27	346	0.07803
WT	4.7 hpf	7	10	258	0.03876
WT	4.7 hpf	8	20	234	0.08547
WT	4.7 hpf	9	23	348	0.06609
WT	4.7 hpf	10	17	330	0.05152

WT	4.7 hpf	11	14	303	0.0462
WT	4.7 hpf	12	21	366	0.05738
WT	4.7 hpf	13	26	321	0.081
WT	4.7 hpf	14	13	246	0.05285
WT	4.7 hpf	15	14	254	0.05512
WT	4.7 hpf	16	18	343	0.05248
WT	4.7 hpf	17	35	341	0.10264
WT	4.7 hpf	18	25	340	0.07353
WT	4.7 hpf	19	13	381	0.03412
WT	4.7 hpf	20	15	208	0.07212
WT	4.7 hpf	21	14	365	0.03836
WT	4.7 hpf	22	18	227	0.0793
WT	4.7 hpf	23	33	342	0.09649
WT	4.7 hpf	24	22	305	0.07213
WT	4.7 hpf	25	13	307	0.04235

Table S2. *In-situ* hybridization statistics for rescue assays. Related to main text and Fig. 6.

in-situ probe/stage genotype treatment	eomesa 6 hpf			mxtx2 4.3 hpf			sox32 8 hpf			sox17 8 hpf		
	stain	no stain	n total	stain	no stain	n total	stain	no stain	n total	stain	no stain	n total
WT	0	42	42	18	0	18	8	0	8	6	0	6
MZ*nanog*	19	0	19	0	20	20	6	2	8	9	5	14
MZ*nanog* plus *mxtx2* mRNA							10	0	10	13	0	13
MZ*nanog* plus miR-430	5	14	19				13	2	15	19	2	21
MZ*nanog* plus miR-430 mism	14	0	14									
MZ*nanog* plus *nanog* mRNA				20	0	20	14	9	25	16	2	18

Table S3. Cotransplantation of labeled nanog -/- and wild type (+/+) cells

(related to the main text, Fig. 8)

# embryo	# exp.	color (r,g), transpl.order(1,2)		skin		neural		muscle		notochord		placodes		floorplate		beans	
Genotype donor cells		+/+	-/-	+/+	-/-	+/+	-/-	+/+	-/-	+/+	-/-	+/+	-/-	+/+	-/-	+/+	-/-
1	1	2g	1r	5	5	0	0	2	1	6	5	0	3	0	0	0	0
2	1	2g	1r	0	0	0	0	10	2	0	0	0	0	0	0	0	2
3	1	2g	1r	0	5	10	3	4	0	7	0	3	0	1	0	0	0
4	1	2g	1r	5	5	10	0	4	2	0	0	0	0	0	0	0	0
5	1	2g	1r	0	0	6	0	0	3	0	0	5	0	0	0	0	0
6	1	2g	1r	3	7	0	0	10	4	0	0	3	0	0	0	0	2
7	2	1g	2r	0	0	0	0	0	0	0	0	2	0	0	0	1	2
8	2	1g	2r	5	2	3	2	5	0	0	0	0	0	0	0	2	4
9	2	1g	2r	0	0	0	0	0	0	0	0	0	0	0	0	0	1
10	2	1g	2r	0	6	0	0	0	0	0	0	0	0	0	0	0	0
11	2	1g	2r	6	3	0	0	0	0	0	0	0	0	0	0	0	1
12	2	1g	2r	0	15	0	0	0	0	0	0	0	0	0	0	0	2
13	2	1g	2r	3	0	4	0	0	0	2	0	0	0	0	0	0	0
14	2	1g	2r	7	6	0	0	6	0	4	0	0	0	0	0	0	0
15	2	1g	2r	6	4	4	0	4	2	0	0	5	0	0	0	0	0
16	3	2r	1g	10	0	2	0	10	0	0	0	0	0	0	0	0	0
17	3	2r	1g	8	1	1	2	3	0	0	0	0	0	0	0	0	1
18	3	2r	1g	8	0	0	0	1	0	0	0	0	0	0	0	0	1
19	3	2r	1g	0	2	0	0	1	2	0	0	0	0	0	0	0	1
20	3	2r	1g	7	0	6	0	0	0	12	0	0	0	0	0	0	1
21	3	2r	1g	8	2	2	0	0	0	0	0	6	3	0	0	0	0
22	3	2r	1g	0	0	0	1	2	0	0	0	3	2	0	0	0	1
23	3	2r	1g	0	0	0	0	0	0	0	0	0	0	0	0	1	1
24	4	1r	2g	0	0	5	0	0	0	0	0	0	0	0	0	0	1
25	4	1r	2g	3	0	0	0	1	0	6	0	0	0	9	0	0	1

26	4	1r	2g	0	0	0	0	0	0	0	0	4	0	0	0	0	1
27	5	1r	2g	5	0	15	0	4	0	0	0	10	0	9	0	0	0
28	5	1r	2g	0	0	0	0	0	0	0	0	10	0	0	0	0	0
29	5	1r	2g	3	2	0	0	0	0	0	0	0	0	0	0	1	0
30	5	1r	2g	0	0	3	0	0	0	0	0	0	0	0	0	0	0
31	5	1r	2g	5	0	7	0	15	0	0	0	2	0	7	0	0	0
32	5	1r	2g	10	0	5	0	10	0	0	0	4	0	0	0	0	0
33	6	2g	1r	5	0	10	0	14	0	0	0	3	0	0	0	0	0
34	6	2g	1r	7	0	3	0	0	0	2	0	0	1	0	0	0	1
35	7	1r	2g	3	0	0	0	0	0	0	0	0	0	0	0	0	0
36	7	1r	2g	0	5	15	7	0	0	0	0	0	0	0	0	0	0
37	7	1r	2g	10	5	20	0	6	0	0	0	3	0	0	0	0	0
38	7	1r	2g	0	0	4	0	0	0	0	0	0	0	0	0	0	1
39	8	2r	1g	0	0	0	0	5	0	0	0	2	0	0	0	0	0
40	8	2r	1g	15	0	9	0	8	0	0	0	7	0	0	0	0	0
41	9	2r	1g	9	0	10	0	7	0	0	0	0	0	0	0	0	0
42	9	2r	1g	9	0	5	0	0	0	7	0	8	0	3	0	0	0
43	9	2r	1g	6	2	5	0	7	0	0	0	6	0	0	0	0	0
44	9	2r	1g	0	0	10	3	4	0	10	0	0	0	0	0	0	0
45	9	2r	1g	5	0	3	0	3	0	0	0	0	0	0	0	1	0
46	9	2r	1g	0	0	0	0	6	0	3	0	5	0	0	0	0	0
47	10	2g	1r	10	0	5	0	0	0	0	0	10	0	0	0	0	1
48	10	2g	1r	8	0	10	0	3	0	5	0	7	0	3	0	0	2
49	10	2g	1r	10	8	0	2	20	10	0	0	0	0	0	0	0	0
50	10	2g	1r	5	0	0	0	0	0	4	0	10	1	2	0	0	0
51	10	2g	1r	6	5	8	0	20	8	0	0	2	1	0	0	0	0
52	10	2g	1r	15	0	10	0	20	0	0	0	2	0	0	0	0	0

Table S4. Sequences of PCR primers used in this work, 5' to 3'. Related to Materials and Methods.

The following primers were used (5' to 3'):

rpl5bf3	GGGGATGAGTTCAATGTGGAG
rpl5br3	CGAACACCTTATTGCCAGTAG
EGFP_sybr_f1	GCGAGGGCGATGCCACCTAC
EGFP_sybr_r1	CGCCGTAGGTCAGGGTGGTC
her3_f	CACGCTGGTTACAGAAGTTGTCTCA
her3_r	TGTGGTTAAGACCGCTCGTAAGATT
sox2_f	GAACACCAACTCCTCGGGAAACAACC
sox2_r	TGTGCATTTTGGGGTTCTCCTGTG
sox19a_f	ATGAAGTCCGCCGTGCCACC
sox19a_r	CGCCTCTGACCCCGAGACCA
foxD3_f	GCTTTCAGCTCTCAGCTAAGTCCAAG
foxD3_r	ACCCCGATGATGTTTTCTATGCTG
sox3_f	GCCTCGGTGCTGACTGGAAA
sox3_r	GGAGTCCCCCTGGCAAAGAA

Table S5. *In situ* hybridization probes used in this study. Related to Material and Methods, *in situ* hybridization section.

gene name	Ref-Seq	References
bmp2b	NM_131360	Hammerschmidt et al., 1996a
chrd	NM_130973	Miller-Bertoglio et al., 1999
eomesa	NM_131679	this study
foxd3	NM_131290	Onichtchouk et al., 2010
gata5	NM_131235	Reiter et al., 1999
gsc	NM_131017	Schulte-Merker et al., 1994
her3	NM_131080	Onichtchouk et al., 2010
mixer	NM_130940	Henry et al., 1998
mxtx2	NM_001079816	this study
ntl (ta)	NM_131162	Schulte-Merker et al., 1994
sox17	NM_131287	Alexander and Stainier, 1999
sox19a	NM_130908	this study
sox2	NM_213118	Onichtchouk et al., 2010
sox3	NM_001001811	Onichtchouk et al., 2010
sox32	NM_131851	Dickmeis et al., 2001
vent	NM_131700	Kawahara et al., 2000
vox	NM_131698	Kawahara et al., 2000

Table S6. Primers used for cloning the plasmid templates for *in situ* probes (from 5' to 3').

gene name	forward Primer	reverse Primer
eomesa	TCTGTACCCGTCCTATCCCG	AGATCCTGTTTGGTGGTCGC
mxtx2	CTCAATGAAAGACATGTGGACTG	CTCTGTAGGTTATGGATGTTTGC
sox19a	GCTGAAAAAGGACAACCCGGCTGC	TTTCCTGATCAGATGTGTGTGAGAGG

Supplementary References

Alexander, J. and Stainier, D. Y. (1999) A molecular pathway leading to endoderm formation in zebrafish, *Current biology : CB* 9(20): 1147-57.

Dickmeis, T., Mourrain, P., Saint-Etienne, L., Fischer, N., Aanstad, P., Clark, M., Strahle, U., and Rosa, F. (2001). A crucial component of the endoderm formation pathway, CASANOVA, is encoded by a novel sox-related gene. Genes Dev. 15, 1487–1492.

Hammerschmidt, M., Pelegri, F., Mullins, M. C., Kane, D. A., van Eeden, F. J., Granato, M., Brand, M., Furutani-Seiki, M., Haffter, P., Heisenberg, C. P., Jiang, Y. J., Kelsh, R. N., Odenthal, J., Warga, R. M., Nusslein-Volhard, C. (1996) dino and mercedes, two genes regulating dorsal development in the zebrafish embryo. *Development* 123: 95-102.

Henry, G. L. and Melton, D. A. (1998) Mixer, a homeobox gene required for endoderm development, *Science* 281(5373): 91-6.

Kawahara, A., Wilm, T., Solnica-Krezel, L., and Dawid, I. B. (2000) Functional interaction of *vega1* and *goosecoid* homeobox genes in zebrafish. *Genesis* 28: 58-67.

Kawahara, A., Wilm, T., Solnica-Krezel, L., and Dawid, I. B. (2000) Antagonistic role of *vega1* and *bozozok/dharma* homeobox genes in organizer formation. *Proc Natl Acad Sci U S A* 97(22): 12121-12126.

Miller-Bertoglio, V., Carmany-Rampey, A., Fuerthauer, M., Gonzalez, E. M., Thisse, C., Thisse, B., Halpern, M. E., Solnica-Krezel, L. (1999) Maternal and zygotic activity of the zebrafish *ogon* locus antagonizes BMP signaling. *Dev. Biol*. 214: 72-86.

Onichtchouk, D., Geier, F., Polok, B., Messerschmidt, D. M., Mossner, R., Wendik, B., Song, S., Taylor, V., Timmer, J. and Driever, W. (2010) Zebrafish Pou5f1-dependent transcriptional networks in temporal control of early development, *Molecular systems biology* 6: 354.

Reiter, J. F., Alexander, J., Rodaway, A., Yelon, D., Patient, R., Holder, N. and Stainier, D. Y. (1999) Gata5 is required for the development of the heart and endoderm in zebrafish, *Genes & development* 13(22): 2983-95.

Schulte-Merker, S., van Eeden, F. J., Halpern, M. E., Kimmel, C. B. and Nüsslein-Volhard, C. (1994) no tail (ntl) is the zebrafish homologue of the mouse T (Brachyury) gene, *Development* 120(4): 1009-15.

Schulte-Merker, S., Hammerschmidt, M., Beuchle, D., Cho, K. W., De Robertis, E. M., and Nusslein-Volhard, C. (1994) Expression of zebrafish *goosecoid* and *no tail* gene products in wild-type and mutant *no tail* embryos. *Development*. 120(4): 843-852.